

A Multiobjective Evolutionary Approach Based on Graph-in-graph for Neural Architecture Search of Convolutional Neural Networks

Yu Xue[†]

1. School of Computer and Software, Nanjing University of Information Science and Technology, Nanjing, China
 2. Engineering Research Center of Digital Forensics, Ministry of Education, Nanjing University of Information Science and Technology, Nanjing, China
- E-mail: xueyu@nuist.edu.cn

Pengcheng Jiang[†]

School of Computer and Software, Nanjing University of Information Science and Technology, Nanjing, China
E-mail: pcjiang@nuist.edu.cn

Ferrante Neri*

COL Laboratory, School of Computer Science, University of Nottingham, Nottingham, UK
E-mail: ferrante.neri@nottingham.ac.uk

Jiayu Liang

Tianjin Key Laboratory of Autonomous Intelligent Technology and System,
Tiangong University, Tianjin, China
Email: yyliang2012@hotmail.com

With the development of deep learning, the design of an appropriate network structure becomes fundamental. In recent years, the successful practice of Neural Architecture Search (NAS) has indicated that an automated design of the network structure can efficiently replace the design performed by human experts. Most NAS algorithms make the assumption that the overall structure of the network is linear and focus solely on accuracy to assess the performance of candidate networks.

This paper introduces a novel NAS algorithm based on a multi-objective modeling of the network design problem to design accurate Convolutional Neural Networks (CNNs) with a small structure. The proposed algorithm makes use of a graph-based representation of the solutions which enables a high flexibility in the automatic design. Furthermore, the proposed algorithm includes novel ad-hoc crossover and mutation operators. We also propose a mechanism to accelerate the evaluation of the candidate solutions. Experimental results demonstrate that the proposed NAS approach can design accurate neural networks with limited size.

Keywords: Deep Learning, Neural Architecture Search, Multi-objective Optimization, Genetic Algorithm.

1. Introduction

Convolution neural networks (CNNs) have achieved remarkable results in solving many prob-

lems, such as image classification¹⁶ and image segmentation⁴⁰. CNNs are very efficient at obtaining features from 1-D sequences of data, 2-D images,

[†]: These authors contributed equally to this work and should be considered *co-first* authors

and 3-D images. The features extracted from 1-D sequences of sound data by 1-D convolution neural networks can be used to extract voiceprint features^{96; 48}. The features extracted from 2-D image data by convolution neural network can be used for image content recognition, prediction, and segmentation. The features in 3-D space in 3-D image data (mostly medical image data) can be extracted by 3-D convolution kernels, which is very useful in predicting diseases and identifying lesions^{35; 34}. In addition, video data with time attributes can also be classified by 3-D convolutional neural networks^{21; 73}.

Among the plethora of real-world applications of CNNs, some modern examples representing the state-of-the-art in the field of neural systems are to analyse the electroencephalogram signals to diagnose seizures^{2; 46; 42} or depression³. A neural system based on multiple CNNs is proposed in Ref.⁵² to control epileptic seizures. Other studies propose CNNs to diagnose epilepsy in infants⁷ and children⁴³ by classifying electroencephalogram signals. CNNs have been also successfully used to classify medical images to diagnose Parkinson's disease^{54; 12} and detect pupils⁷². Another popular application domain for CNNs is civil engineering. Some examples of application include damage detection in concrete structures³⁹ and roads⁵³. Some other examples are about vibration-based structural state identification⁹⁵ and effect of wind on structures⁵⁹. In addition, CNNs can be combined with other technologies to be applied in more fields. In Ref.⁵⁶ CNNs are combined with Long Short Term Memory to accurately predict the remaining useful life of components, thus helping to make an optimal decision for maintenance management.

There have been many classical network structures, such as Alexnet³⁶, VGG⁷⁴, GoogLeNet⁸⁴, Inception-V4⁸³, Inception-Resnet⁸³, Resnet³¹, Densenet³³, etc., which appear to perform well in image classification and image segmentation. However, due to high complexity, it is impractical to use these CNNs on mobile platforms since they would require an excessive amount of computational resources thus leading to an unreasonable waiting time, memory overflow, and high energy consumption. Therefore, some new lightweight network structures for mobile platforms have been proposed, such as MobileNet⁶⁸, ShuffleNet⁵¹, MnasNet⁸⁵, EfficientNet⁸⁶, Xception¹⁹, etc. All the net-

work structures mentioned above are the result of (human) expert design.

In recent years, Neural Architecture Search (NAS) methods¹⁷, that automatically search the network architectures, are progressively becoming more popular to design CNNs. Most NAS methods are to search the blocks or cells which are consist of convolution kernels with different sizes (such as 3×3 , 5×5 , etc.) and the position of pool layers^{50; 82; 80}. Moreover, in MUXConv⁴⁹ and ShuffleNet⁵¹, it is pointed out that the generalization performance of the network can be improved by channel multiplexing, spatial multiplexing, and channel shuffling, and then the accuracy of recognition can be improved. The majority of the NAS methods in the literature perform the automatic design by using accuracy as the sole objective of the targets. However, operational efficiency is also an extremely important aspect of the functioning of the network, especially in mobile applications.

In order to simultaneously address accuracy and computational cost, unlike the other studies in the literature, we propose an encoding mechanism with multi-objective evaluate mechanism of the problem where besides the accuracy of the CNN also the number of network parameters is taken into consideration^{65; 66; 75; 88; 69; 70}.

Existing NAS methods design and limit the search space and search domain to reduce the time complexity of the optimization problem. An usual strategy consists of defining some building blocks which are defined by a human expert. This study proposes a graph-based flexible representation that supports a higher level of automatism of the design process. Furthermore, the proposed method relates to the concept of regularized evolutionary algorithm^{67; 62} in that the approaches aim at reducing the computational overhead (e.g. memory employment) by performing an action on the optimization algorithm.

The remainder of this paper is organised in the following way. Section 2 provides the background about NAS methods, encoding mechanism and evaluation of candidate network architectures. Section 3 provides the details of the proposed NAS method. Section 4 provides the numerical results of this study.

2. Related Work: Neural Architecture Search

The majority of NAS methods can be categorised according to their search logic:

- Gradient-based methods^{47; 92; 15;}
- Reinforcement Learning (RL)^{98; 28; 9;}
- Evolutionary Algorithms (EA)^{79; 50; 91; 63, 82.}

This list does not mean to be exhaustive since other methods not belonging to any of the categories above exist, such as Monte Carlo Tree search⁹⁰. The various NAS methods belonging to each category above present advantages and disadvantages. Specifically, RL-based algorithms require a large computational time to perform the automatic design, even on median-scale datasets, such as cifar10 and cifar100³⁷. Unlike RL-based algorithms, gradient-based algorithms are usually very fast. Besides, their search logic leads to obtaining a local optimum problem which may have a much poorer performance than the desired optimal design. Moreover, the gradient-based search algorithm needs to construct a super network in advance, which should contain as much search space as possible. The construction of this super network requires substantial human intervention of an expert, see Ref.^{15; 25}. Although EAs are not theoretically guaranteed to converge to the global optimum of problem, they are able to overcome the local optima. Also, they do not require a super network. Thus, EAs are often considered a viable compromise for NAS since they are relatively fast and can be applied to NAS without human intervention or prior knowledge of the problem. One pioneering example is in Ref.⁹⁴. It is worthwhile remarking that there exist other search strategies integrated in NAS methods such as Ref.⁵⁷, Ref.¹⁸, and Ref.⁵⁵.

This paper focuses on EAs for NAS. In the following subsections, some context is provided around the two major challenges of this approach: encoding mechanism and evaluation of the candidate solutions.

2.1. Encoding of NAS

The encoding of candidate network architectures for NAS methods are broadly divided into two categories³⁸: direct encoding and indirect encoding. Indirect encoding was often used in early

works on NAS usually referred to as *Neuroevolution*, see Ref.⁷¹, which is similar to NAS. Neuroevolution uses evolutionary computation to optimize the structure and parameters of neural networks at the same time^{4; 27; 30; 26; 1}, and many researchers still work on it^{76; 77; 64; 32; 8}. However, due to the limitations of equipment at that time, the neuroevolution can only be performed on small networks. Furthermore, due to the very large number of parameters in fully connected networks, direct encoding cannot be used to represent the whole network. Therefore, a lot of effort is made to find simple ways (*i.e.*, indirect encoding) to represent the connections and weight parameters of neurons. Thus, indirect encoding is a popular strategy to simplify the search space. These search purposes determine that search space is difficult to represent with direct encoding, so indirect encoding is needed to simplify the encoding and early researchers used indirect encoding to represent individuals.

In recent years, most of the NAS studies have been conducted on neural networks that albeit complex, can be naturally schematised as interconnected blocks. This is the case, besides the CNNs, of Generative Adversarial Networks (GANs)²⁸, and Recurrent Neural Networks (RNNs)⁴⁷. For networks of these types, direct encoding is an easy and natural option. For example, CNNs contain convolution blocks, pooling blocks, batch normalization operations, and sometimes activation functions. These blocks are often represented by a few parameters. Convolution blocks can be fully represented by the number of convolution cores, the size of the convolution cores, stride, padding, dilation and groups (in fact, some parameters can be directly ignored based on the actual search strategy and purpose). In most cases, pooling blocks, batch normalization operations and activation functions do not even require parameters for special representations, and they just need the position in the structure to represent the modules.

For each block's position in the structure, there exist two encoding mechanisms

- linear structure⁸¹, that is the sequential (linear) arrangement of all blocks or units composed of blocks;
- graph structure⁹¹, that is a planar (graph) arrangement of interconnected blocks.

Although formally a linear structure is a special graph structure (a sequence is a special graph), we emphasise the distinction since the two encoding mechanisms correspond to two significantly different implementations.

Adjacency matrices are better suited for dense graph structures⁵⁸, since sparse structures can waste a lot of space in adjacency matrices. Sparse structures are better represented by adjacency tables (or adjacency lists). While adjacency matrices are matrices of '0' and '1' to indicate connection or without connection between nodes, adjacency tables are lists that indicate the for each node which nodes are linked to it. The latter allows a compact representation of large sparse networks.

The main advantage of a linear structure is its simplicity compared to that of graph structure. Besides, linear structures cannot represent all the networks. In some cases, like the example in Fig. 1, a linear structure would yield an ambiguous representation of a neural network.

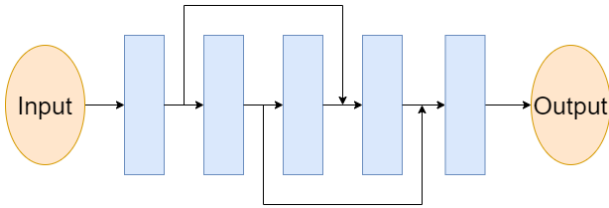


Fig. 1. An example of architecture that cannot be represented by a linear structure. Blue blocks are modules in CNNs. This architecture has two skip connections, so it can't be represented by a linear structure.

2.2. Evaluation of NAS

To evaluate a candidate structure, the general practice is to train the network and calculate its accuracy, see Ref.⁸⁰.

Since the training time of the network is very time-consuming, there are many ways to reduce the total time of the evaluation phase. There are two ways to reduce the total time: foresight and early closure. Foresight methods make use of models to predict the performance of the training network. Some researchers use the performance during training to predict the future performance. For example, MetaQNN¹⁰ gives the first 25% of the historical data of the Stochastic Gradient Descent (SGD) training curve to the time series model for prediction and estimates the final accuracy of the network structure. Some researchers use other models, such

as random forest, Bayes methods or other models to predict the possible representations of particular network architectures. The reason why they use this method is that the structures searched for by the same NAS method often have a great deal of similarity, and when encoded, it is possible to work out whether the network is good or not from the encoding directly. For instance, PNAS⁴⁵ uses the model to predict the top-1 accuracy of candidate networks. Ref.⁷⁸ proposes an end-to-end offline performance predictor based on the random forest to accelerate the evaluation.

Early closure is another way to reduce the total time of the evaluation phase. This type of approach reduces overall time through targeted evaluations. For example, many researchers used subsets of the dataset for training^{99; 89}, so that the time of training each network will decrease. Also, Ref.⁸⁹ uses a strategy to identify the required structure in advance. In ChamNet²⁰, only 300 high-accuracy (or other indicators) samples with different efficiency are selected for each training. Another approach is to keep the good structure and weight so that the new structure requires fewer times to train. There are three specific implementations of this approach: weight sharing, One-Shot method, and weight inheritance. The weight sharing method, which is mostly used in NAS based on gradient, makes use of shared weights from a super network to accelerate the training process, see Ref.^{47; 92; 15; 98; 50}. The one-shot method consists of adding components to a small network or deleting components from a large network^{41; 22; 29; 11}. The weight inheritance method is mostly used in NAS based on EAs^{63; 23; 14; 24}. This method requires that the candidate networks of the entire search space have similar structures. Most of the network structures found by NAS based on EAs meet this condition.

Figure 2 illustrates the weight inheritance method. In the upper part of the figure, two parent solutions with a crossover point (indicated as a diamond) are depicted. The first parent solution is composed of the sequences G_1 and G_2 (representing the network structure) with the corresponding weights W_1 and W_2 . Analogously, the second parent solution is composed of G_3 and G_4 with the weights W_3 and W_4 . In the lower-left part of the figure, the standard crossover is illustrated. The sequences G_2 and

G_4 are swapped over and four sets of corresponding weights W_5, W_6, W_7 and W_8 are randomly initialized, thus generating new networks (indicated with a darker colour). In the lower right part of the figure, the weight inheritance method is illustrated. When the crossover occurs, the offspring solutions inherit the weights of the parent (the weights of that portion of the network). Thus, the first offspring solution is composed G_1 and G_4 with the weights W_1 and W_4 while the second solution is composed of G_3 and G_2 with the weights W_3 and W_2 .

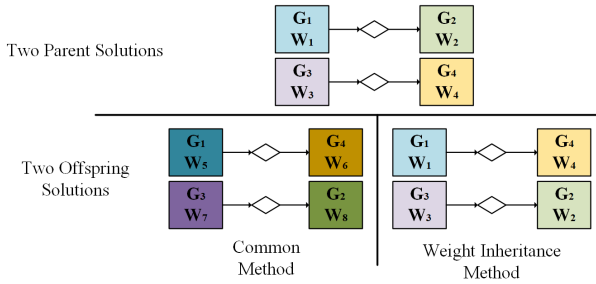


Fig. 2. Comparison between basic crossover (with random initialization of the weights) and crossover with weight inheritance method.

3. The Proposed Approach: MOGIG-Net

In this section, we introduce the framework of the proposed NAS algorithm, namely Multi-Objective Graph-in-graph Network (MOGIG-Net) whose flowchart is shown in Fig. 3.

This section firstly introduces the overall framework of the proposed algorithm and then describes the encoding mechanism, crossover, mutation, decoding method, evaluation, and environment selection in details.

3.1. Overall Description of the MOGIG-Net Framework

Fig. 4 displays the structure of the whole algorithm. First, the initial population is obtained through random initialization (line 1), and then the fitness evaluation of the initial population is calculated (line 2-3).

After the initialization, the algorithm makes use of generation cycles to process the population (line 4-15). New individuals are generated through crossover and mutation. The new individuals are selected for the survival of the fittest by evaluating the fitness values for each objective (line 12-13). Finally,

individual sets with better performance on multiple objectives are obtained.

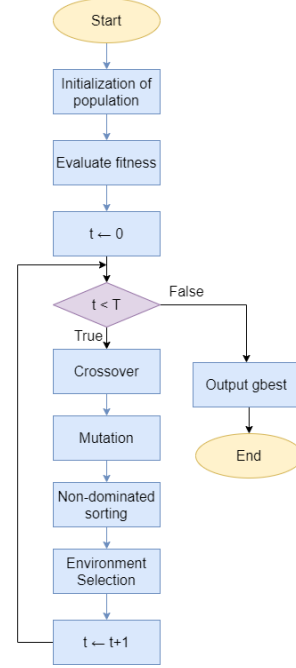


Fig. 3. Flowchart of the of the MOGIG-Net framework

Input: The population size p , the maximal generation number T , the crossover probability μ , the mutation probability ν , the maximal nodes number in each block (M_{min}, M_{max}), the maximal blocks number (N_{min}, N_{max}).
Output: Collection of individuals on the pareto frontier meeting the minimization goals.

- 1: $P_0 \leftarrow$ Initialize a population with the size of p by using the proposed encoding strategy in Algorithm 6;
 - 2: Convert all genes in P_0 to models and evaluate the fitness of the models by method 12, and record the fitness of each corresponding individual;
 - 3: Record the fingerprint and fitness value of each individual.
 - 4: $t \leftarrow 0$
 - 5: **while** $t < T$ **do**
 - 6: $Q \leftarrow \phi$
 - 7: **if** the length of $Q < P$ **then**
 - 8: Two individuals were randomly selected and will cross and mutate by the method of Algorithm 7 and 8, and then two offspring will be generated.
 - 9: Record the fingerprint of each offspring, and add the two offspring into population Q .
 - 10: **end if**
 - 11: $P_t \leftarrow P_t \cup Q$
 - 12: Convert genes to models and evaluate the fitness of individuals in Q by method 12 to control sequence, and record the fitness of each individual;
 - 13: Sort P_t by non-dominated sorting algorithm, and retain P individuals with better performance, and delete other individuals with poor performance, then we will get P_{t+1} ;
 - 14: $t \leftarrow t + 1$
 - 15: **end while**
- Return:** P_{T-1}

Fig. 4. Framework of the MOGIG-Net algorithm

In NAS problems, the evaluation phase is by far

340 the computationally most expensive as it requires
 341 the training of the candidate network structure. In
 342 order to avoid the re-evaluation of the same archi-
 343 tectures/structures, we keep an archive of visited
 344 solutions with their objective function value. If a so-
 345 lution is re-visited the archived objective function
 346 values are used.

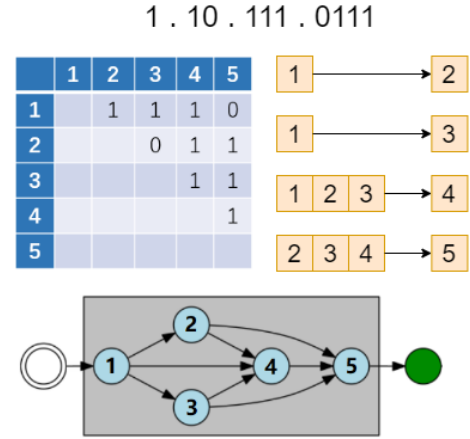
347 3.2. Encoding Mechanism of MoGIG-Net

348 In this study, we use a graph structure to encode the
 349 architecture of the network. We propose the encod-
 350 ing of a CNN in a chromosome divided into blocks
 351 linked by separators. To understand the proposed
 352 encoding, let us remark that CNNs are composed
 353 of blocks, three of them being essential and named
 354 1) convolution; 2) pooling; 3) fully connection. The
 355 chromosome representing the CNN is described as
 356 follows:

$$357 \quad \text{CB}_1\text{-CB}_2\text{-}\dots\text{-CB}_n\text{-S-P}$$

358 where each CB_j is a convolution block, **S** represents
 359 the structure how the convolution block are inter-
 360 linked and **P** describes the presence of pooling lay-
 361 ers in the CNN.

362 The convolution block CB_j is a sequence of sep-
 363 arators and binary numbers. The '1' indicates a link
 364 between neurons while '0' indicates the dismiss a
 365 connection. A convolution block containing m neu-
 366 rons is represented by a sequence of $\frac{m(m-1)}{2}$ binary
 367 numbers grouped in sub-blocks of $1, 2, \dots, m-1$ bi-
 368 nary numbers. Each sub-block is separated by a dot.
 369 This sequence of binary numbers is the adjacency
 370 matrix associated with the convolution block. More
 371 specifically, each sub-block contains the information
 372 of a column of the adjacency matrix. Fig. 5 provides
 373 an example of the proposed encoding for $m = 5$.
 374 On the top of the figure, the encoding used in this
 375 study is shown. Below the chromosome, the corre-
 376 sponding adjacency matrix and table are displayed.
 377 It may be noticed that each block of the chromosome
 378 contains the columns of the adjacency matrix. At the
 379 bottom of Fig. 5, the corresponding network struc-
 380 ture is represented. Also, like CB_j representing the
 381 connections in each block, the binary numbers in **S**
 382 is also the same representation as CB_j , and thus rep-
 383 resents the connection between blocks.



384 Fig. 5. Encoding of a convolution block CB_j (part of the chromosome) of the candidate CNN. The corresponding adjacency matrix and table are displayed as well as the graph of the encoded network. Convolution blocks formed by these binary blocks are the components of the CNN

385 The structure S is also a sequence of binary
 386 numbers which has $\frac{n(n-1)}{2}$ bits. The 1 indicates a
 387 link between two convolution blocks CB_i and CB_j
 388 while 0 indicates the dismiss of connections be-
 389 tween blocks. The sequence S is also divided into
 390 sub-blocks composing the columns of the adjacency
 391 matrix that describes the topology of the intercon-
 392 nections among convolution blocks. The sequence
 393 P is composed of n binary numbers, one for each
 394 convolution block CB_j composing the CNN. The se-
 395 quence P can be seen as a binary sequence Z where
 396 $z_j = 1$ represents the presence of pooling layers (P_j
 397 in Fig. 9) pointing to CB_{j+1} while $z_j = 0$ represents
 398 the absence of a pooling layer pointing to CB_{j+1} .
 399 The last binary number z_n indicates the presence or
 400 the absence of a pooling layer between CB_n and the
 401 fully connected layer FC.

402 Fig. 6 provides the implementation details of
 403 the encoding mechanism in the context of the ini-
 404 tialization of the population to be processed by
 405 MOGIG-Net.

406 The chromosome code only contains the topo-
 407 logical structure before the fully connected layer.
 408 The connection mode between the components of
 409 each individual is determined at the beginning
 410 of the algorithm (residual connection³¹ and close
 411 connection³³).

412 Let us indicate with α the maximum number of
 413 cells of and with β the maximum number of blocks

of the CNN. The longest possible code to search for contains L bits, and L is calculated by the following formula.

$$L = \frac{\alpha(\alpha - 1)}{2} + \frac{\beta(\beta - 1)}{2} + \alpha$$

The search space contains up to 2^L possible candidate networks.

Input: The limit of nodes number in each block (M_{min}, M_{max}), the limit of blocks number (N_{min}, N_{max}), the maximal pooling blocks number K .
Output: One chromosome

- 1: Generate a random number $n, n \in (N_{min}, N_{max})$;
- 2: $flag \leftarrow 0$
- 3: $gene \leftarrow$ empty string
- 4: **while** $flag < n$ **do**
- 5: Generate a random number $m, m \in (M_{min}, M_{max})$;
- 6: Generate a random sequence s of $\frac{m(m-1)}{2}$ binary numbers and allocate them with "." separators in CB_{flag}
- 7: Make sure that the sequence represents a connected graph, see Fig. 10.
- 8: $gene \leftarrow gene + s + ' - '$, the '-' in this paper is the separator between genes of blocks and pools
- 9: $flag \leftarrow flag + 1$
- 10: **end while**
- 11: Generate a random sequence s of $\frac{n(n-1)}{2}$ numbers and allocate them with "-" separators in **S**.
- 12: Make sure that the series can represent an oriented connected graph, see Fig. 10.
- 13: Generate a random sequence p of n binary numbers and allocate them in **P**
- 14: $gene \leftarrow gene + s + ' - ' + p$

Return: chromosome

Fig. 6. MOGIG-Net Encoding Strategy and Initialization

3.3. Crossover and Mutation

Due to the encoding mechanism proposed in this paper, an ad-hoc crossover operator is here proposed to ensure that the offspring solutions meaningfully represent structures of neural networks¹³. Furthermore, a meaningful chromosome must represent a connected graph.

The proposed crossover operator combines two chromosomes I and II by selecting randomly some blocks from the first and then filling the missing gaps with the genotype of the second to ensure that the offspring is meaningful. Fig. 7 provides the implementation details of the crossover.

For the chromosome I, two separators are randomly selected. Then the number of separators n between the two selected separators is calculated (line 6). Then, two separators in the chromosome II are selected while the number of separators between these two separators is ensured to be also n (line 7). Finally, the genes between the two separators are exchanged (line 8).

The mutation operation, outlined in Fig. 8, consists of the random flip from 0 to 1 or from 1 to 0 of a gene (except for the position of separator). Although the location of mutation changes is limited, the fact is that only small connection changes will affect all the input feature maps after this.

Input: Two parents, p_1 and p_2 , probability of crossover $\mu \in (0, 1)$.
Output: Two offspring, q_1 and q_2 .

- 1: Generate a random number $flag$;
- 2: **if** $flag > \mu$ **then**
- 3: **if** num of separators in $p_1 >$ num of separators in p_2 **then**
- 4: $p_1, p_2 \leftarrow p_2, p_1$
- 5: **end if**
- 6: Select two different positions of separator randomly, l_1 and l_2 , in p_1 , (suppose $l_1 < l_2$);
- 7: Select two different positions of separator randomly, l_3 and l_4 , in p_2 , and make sure that the num of separators in $p_1[l_1 : l_2]$ is the same as the num of separators in $p_2[l_3 : l_4]$;
- 8: Exchange the parts $p_1[l_1 : l_2]$ and $p_2[l_3 : l_4]$, then get two offspring, q_1 and q_2 ;
- 9: **else**
- 10: $q_1 \leftarrow p_1$;
- 11: $q_2 \leftarrow p_2$;
- 12: **end if**

Return: q_1 and q_2 .

Fig. 7. MOGIG-Net Crossover

Input: One individual, p , probability of mutation $\nu \in (0, 1)$, bits to change, n .
Output: One individual, q .

- 1: Generate a random number $flag$;
- 2: **if** $flag > \nu$ **then**
- 3: $q \leftarrow$ modify n different bits in q ;
- 4: **else**
- 5: $q \leftarrow p$;
- 6: **end if**

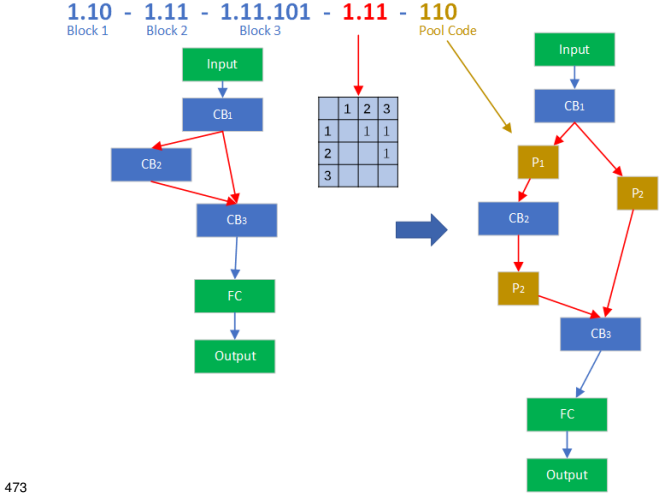
Return: q .

Fig. 8. MOGIG-Net Mutation

3.4. Decoding of MOGIG-Net

Fig. 9 represents the construction of the CNN from its chromosome. At first, the CB_j (in blue) are decoded. If the CB_j is the same as that in the corresponding position in its parents, the module is copied from its parents. Otherwise, the module is generated according to the procedure illustrated in Fig. 5. Then, the **S** is decoded and the corresponding connection is represented by an input array of each block (such as the two red arrows pointing to CB_3). Finally, **P** is decoded and the corresponding position in each input array of each block is wrapped by an adaptive pooling (like the right sub-figure in 9). The connection method in the detailed structure depends on the method which we choose before the

algorithm. If we use the residual structure, we add the connection directly. If we use the dense structure, we adjust the channel and merge it by using the 1x1 convolution kernels to a unitize the channel number.



473

Fig. 9. Construction of a CNN from its chromosome: The blocks or connections are decided by the part of encoding in the same colour. The green squares represent fixed structures. FC means a fully connected layer. P means a pooling layer. Blocks are built in Fig. 5

We also implemented a mechanism to handle missing connections within and among blocks when an adjacency list is generated. Let us consider at first the nodes within a block. If the generated solution contains a node which has inputs and no outputs, then a link between the node and the output node of the block is created. If the generated solution contains a node which has outputs and no inputs, then a link from the input node is generated. If a node has neither inputs nor outputs, then the node is removed. The same reasoning is performed about the connectivity among blocks where each node represents a block while input and output blocks of the CNN are considered instead of input and output nodes of the block. Figure 10 describes this mechanism by showing the three possible scenarios where node 3 has only inputs (left), has only outputs (centre), has neither inputs nor outputs.

During the construction of a CNN from its chromosome, the skip connections (in blocks and between blocks), which need the sizes of the input and output to be the same, are fundamental to achieve a graph structure network. However, con-

497

volution and pooling operations can both change the size of the image. This characteristic of CNNs makes difficult to unify the input size of each part in the graph structure network. Therefore, we maintain the size consistency in the input and output of each block or search unit, so that the size reduction is completely controlled by the pooling layer. It is simple to keep the image size unchanged in the convolution block, only by adjusting the super parameters of the convolution kernel and avoiding the use of a pooling layer.

The formula for calculating the size of input and output is given in Eq.(1), where X_{out} and X_{in} are the size of the input and output, p is the number of padding around the input, d is the offset of two adjacent points of the dilated convolution, k is the size of the convolution kernel, and s is the step size of the convolution operation. Therefore, the size is controlled by means of the convolution kernel.

$$X_{out} = \left\lfloor \frac{X_{in} + 2 \times p - d \times (k - 1) - 1}{s} + 1 \right\rfloor \quad (1)$$

Furthermore, since maintaining the consistency of image size outside the convolution block (i.e., the macro structure) another countermeasure has been adopted. We also encode the reduced position of the size (but did not add into the genes) as the reduction of the size does not affect the use of convolution kernel, see Fig. 6 line 11.

We chose adaptive pooling, which is different from the traditional pooling operation. This operation can dynamically create pooled cores according to the input and output requirements, and it has been used in the last layer of many existing models^{31; 33}. The step size of the adaptive pooling layer can be obtained by Eq (2)

$$stride = \left\lfloor \frac{size_{in}}{size_{out}} \right\rfloor \quad (2)$$

where $size_{in}$ is the size of input feature map and $size_{out}$ is the size of output feature map. The size of pool $size_{pool}$ is then calculated in Eq (3)

$$size_{pool} = size_{in} - stride * (size_{out} - 1) \quad (3)$$

On the basis of these two formulas, we can adjust the kernel of the adaptive pooling layer from the size of the input feature map and the size of the desired output feature map. As shown in Fig. 11, the two pool layers before the block and FC marked in

541

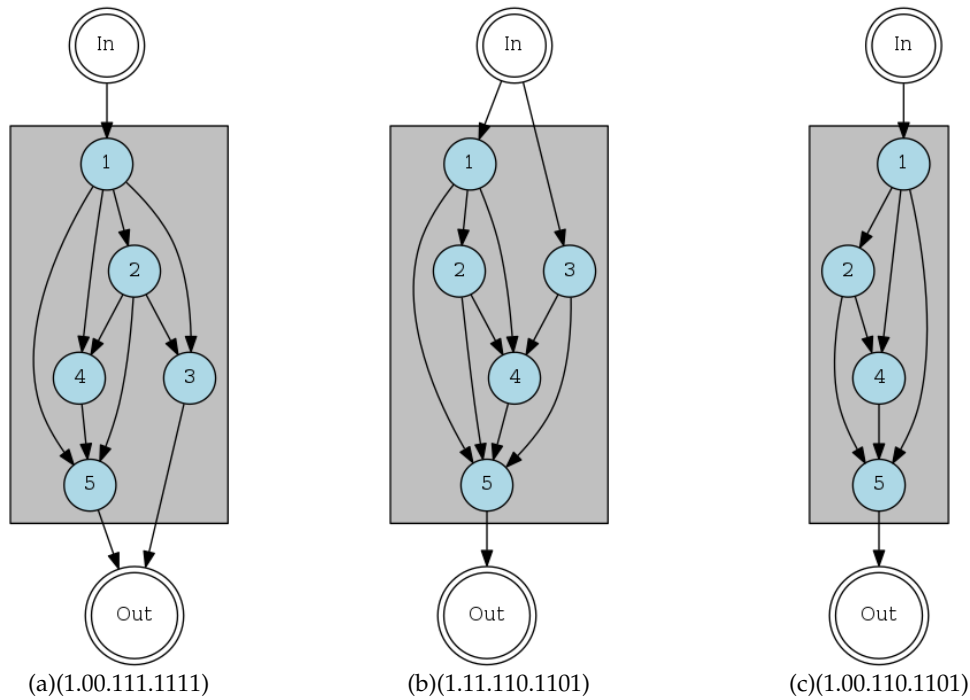


Fig. 10. Three scenarios to guarantee connected CNN blocks. In the left encoding, node 3 would have only inputs. Thus, an output link is generated to guarantee connectivity. In the central encoding, node 3 would have only outputs. Thus, an input link is generated to guarantee connectivity. In the right encoding, node 3 would be isolated. Thus, the node is removed from the graph.

bold because we choose to add adaptive pools before them. In this way, we can control the size of input and output in each layer by controlling the position of adaptive pooling. The location of adaptive pooling and the combination of these channels are referred to as the detailed structure of the individual and are recorded separately.

3.5. Evaluation and Environment Selection

We divide the training sets D into two parts, 80% of which are real training sets D_{train} , and the rest are validation sets D_{valid} . When the new population of offspring solutions is generated, their performance must be assessed to select the population undergoing the following generation. The networks composing the new population undergo training by means of the training set D_{train} . When the change range is below a pre-arranged threshold, the learning rate is adjusted accordingly. If the learning rate adjustment is less than a prearranged value, the training will be stopped.

In our approach, we use weight inheritance to speed up the search. Since our crossover operation can en-

sure that most of the modules of the network remain unchanged, the weight of the model constructed by the child will directly inherit the weight from the model of the parent. This method, like weight sharing, can make the network model obtain a relatively high accuracy rate at the early stage of evolution. In this way, we only need to continue training at a relatively small learning rate to achieve the best performance of each network.

After the training, the accuracy $q.acc$ (that is the error rate) of the network is assessed by means of the validation set D_{valid} . Furthermore, the model size in terms of the number of parameters $q.params$ is also calculated. Both the scores $q.acc$ and $q.params$ characterise the quality of the candidate CNN. The non-dominated sorting⁵⁰ is used to select among parent and offspring solutions the population undergoing the following generation, which often used to evaluate the quality of two solutions in the process of multi-objective optimization⁹³. The condition for one individual to dominate another is to have a performance not worse than the other according to all objective and

542
543
544
545
546
547
548
549
550
551
552
553
554
555
556
557
558
559
560
561
562
563

564
565
566
567
568
569
570
571
572
573
574
575
576
577
578
579
580
581
582
583
584
585
586

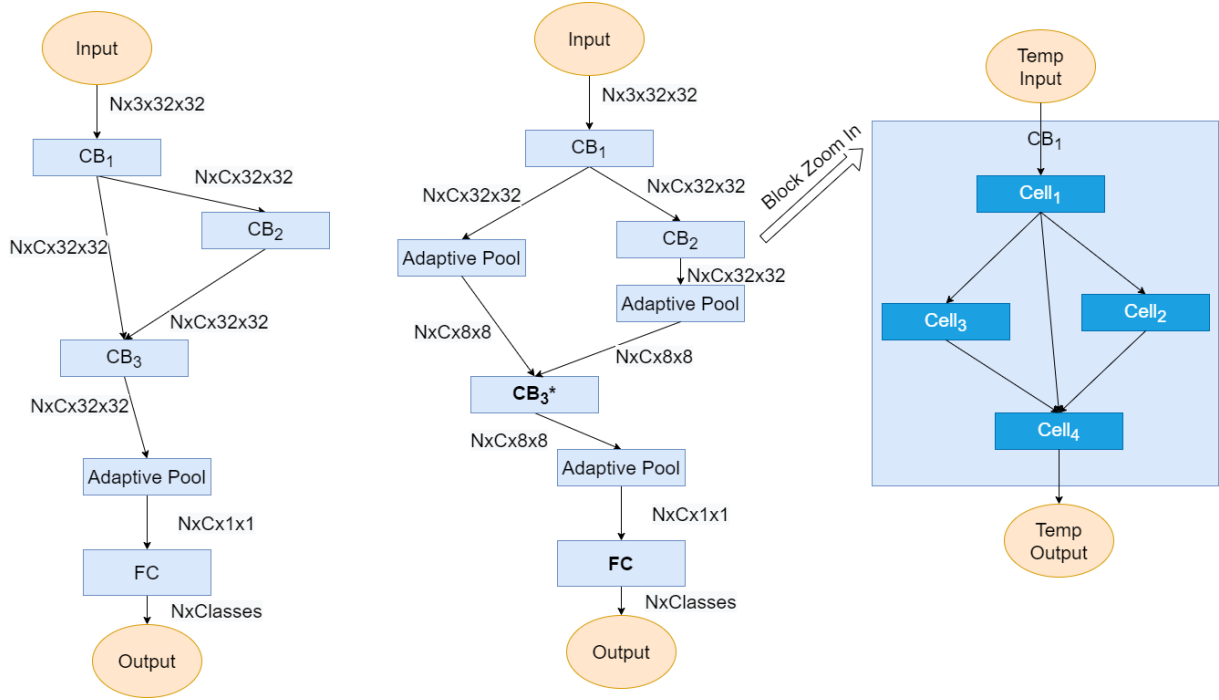


Fig. 11. The left subgraph is the macro structure without pool layers. After executing line 11 of the algorithm in Fig. 6, the adaptive pooling is added at the specified location (center subgraph). The right subgraph is micro structure. Each block includes some convolution cells, and each cell is consist of 3x3 and 1x1 convolution kernels, which do not change the size of input.

587 to outperform it according to at least one objective.

588 Fig. 12 provides the implementation details of
589 evaluation and selection mechanisms.

590

591 3.6. Limitations of MOGIG-Net and 592 Countermeasures

593 Without a prior knowledge on the problem, each
594 connection has initially the same probability to be
595 set as 0 or as 1. Thus, on average initialized solu-
596 tions contain approximately half of the skip connec-
597 tions, many of them being unnecessary. These skip
598 connections can cause a slow down of the network
599 training. Thus, the search efficiency of our method
600 is rather low in the early stages. However, the method
601 of weight inheritance accelerates the search and par-
602 tially mitigates this limitation. Already from the sec-
603 ond generation of the population, we observed a
604 large number of excellent structures in the popula-
605 tion and its parameters are retained along with the
606 encoding, which makes the training process overall
607 efficient and yields high-performance candidate so-
608 lutions.

609 4. Experiments

610 This section displays the results of the proposed
611 MOGIG-Net on two popular datasets and compares
612 its performance with that of seventeen NAS meth-
613 ods previously proposed in the literature.

614

| |
|---|
| <p>Input: The population P_t, the training set D_{train}, the validation set D_{valid}</p> <p>Output: The new population P_{t+1}</p> <ol style="list-style-type: none"> 1: for all individual q in population P do 2: Check the database of fingerprint 3: if fingerprint of q is in the database then 4: Get $q.acc$ and $q.params$ from database; 5: else 6: $cnn \leftarrow$ Generate the network with q; 7: train cnn on D_{train} until the loss and accuracy don't change significantly; 8: $q.acc \leftarrow$ the rate of accuracy assessed on the valid set; 9: $q.params \leftarrow$ the number of parameters contained in the model cnn itself; 10: end if 11: Update individual q in population P; 12: end for 13: Do non-dominated sorting⁵⁰ and select half of the individuals who were better at multiple goals from P_{t+1}. <p>Return: P_{t+1}</p> |
|---|

615

Fig. 12. MOGIG-Net Multi-objective Evaluation and Selection

The popular datasets considered in this study are Cifar-10 and cifar-100 proposed by the Canadian Institute for Advanced Research³⁷. These two datasets are often used to verify the performance of network models. Each dataset comprises 60000 images, including 50000 in the training set and 10000 in the test set. Each image is a 3-channel colour image, and the height and the width are both 32. There are 10 categories in cifar-10 and 100 categories in cifar-100. Both cifar-10 and cifar-100 come from a larger dataset of 80 million small images. Therefore, to a certain extent, cifar-10 and cifar-100 can illustrate the predictive ability of the model.

Table 1 displays the results of MOGIG-Net and twenty-one NAS competitors on cifar-10 and cifar-100. The listed methods are divided into three design categories: NAS human design, single-objective approaches and multi-objective approaches. For each NAS method considered in this study, the reference to its original implementation. For each method we report the result of the objectives in the proposed model, that is the accuracy $q.acc$ expressed in terms to percentage error for Cifar-10 and Cifar-100 and the complexity $q.param$ expressed in million of parameters of the network designed by the corresponding NAS method. We may observe that the proposed MOGIG-Net can efficiently detect networks which combine a relatively low number of parameters and a low percentage error. For example, none of the seventeen competitor NAS methods can achieve an error rate of 14.38% on Cifar-100 with only 3.7 million parameters. With respect to NSGA-Net⁵⁰, that is a recent NAS method considered the state-of-the-art in the field, the proposed MOGIG-Net designed networks with a comparable performance notwithstanding a lower number of parameters (approximately 10% fewer parameters).

Figures 13 and 14 display the solutions in the objective space considered in this study detected by the proposed MOGIG-Net and its competitor. To enhance the readability of the figures, we present a zoom around the non-dominated solutions.

We noticed that when the network structure is relatively large, the number of pooling in the detailed structure greatly affects the required training time and the memory space. When the number of pooling is small and the network structure is large, the size of intermediate variables is very large and

the training time is very long. The results in this study have been detected after two weeks of calculation.

Experimental results show that for networks with similar structures, the accuracy of large models is higher than that of small models, including our method. The reason of this phenomenon is that the increase in the number of parameters appears to improve the generalization capability of the model. Therefore, the maximum accuracy that can be achieved with large models is higher than that of smaller models.

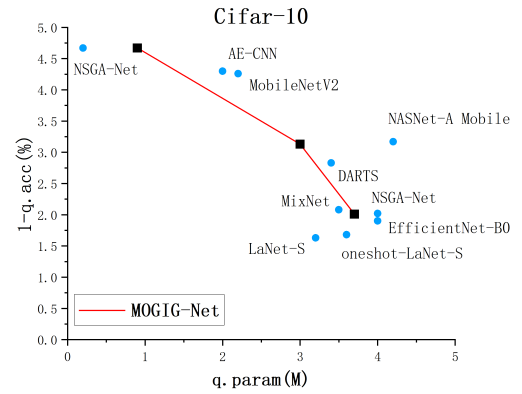


Fig. 13. Solutions detected by MOGIG-Net and its competitors represented in the objective space (Cifar-10)

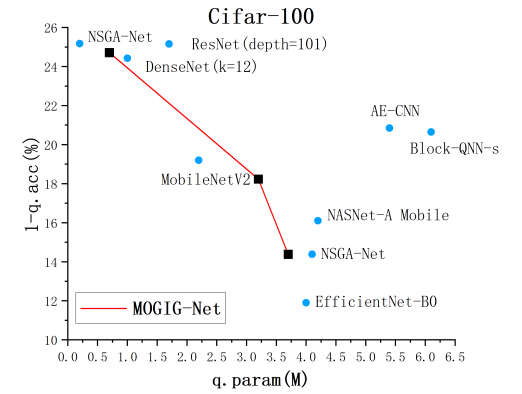


Fig. 14. Solutions detected by MOGIG-Net and its competitors represented in the objective space (Cifar-100)

The results in Fig. 13 and Fig. 14 show that MixNet and MobileNetV2 display excellent performance. However, MixNet and MobileNetV2, unlike the proposed MOGIG-Net are human-designed networks with a predefined purpose. Thus, the per-

684 performance of the methods cannot be directly compared. Also, LaNet produced a solution that dominates the MOGIG-Net solution for cifar-10. We suspect that this may be because LaNet tends to select large models with high accuracy, and we come to this conclusion because some of the networks in the search space, like LaNet-L and oneshot-LaNet-L, seems to be large.

692 However, when the network structure is relatively small, with the increase of total computation times (Multiply-Adds operations), the generalization performance of the network is also improving. Consequently, the next step of this work will be to transform the network structure and/or to determine the number of pooling which is randomly added to the network structure, instead of randomly generating several pooling layers and inserting them into random locations.

702 Table 1. Results on Cifar-10 and Cifar-100 datasets
703 ³⁷ of the proposed MOGIG-Net against **twenty-one**
704 NAS methods. The percentage error “Error Rate (%)” and number of parameters expressed in million pf parameters “Params(M)” are reported.

| Name | Params(M) | Error Rate(%) | |
|-------------------------------------|-----------|---------------|-----------|
| | | Cifar-10 | Cifar-100 |
| Human Design | | | |
| DenseNet(k=12) ³³ | 1.0 | 5.24 | 24.42 |
| ResNet(depth=101) ³¹ | 1.7 | 6.43 | 25.16 |
| ResNet(depth=1202) ³¹ | 10.2 | 7.93 | 27.82 |
| MobileNetV2 ⁶⁸ | 2.2 | 4.26 | 19.20 |
| NASNet-A Mobile ⁹⁹ | 4.2 | 3.17 | 16.10 |
| EfficientNet-B0 ⁸⁶ | 4.0 | 1.90 | 11.90 |
| MixNet ⁸⁷ | 3.5 | 2.08 | - |
| DARTS ⁴⁷ | 3.4 | 2.83 | - |
| VGG ⁷⁴ | 20.1 | 6.66 | 28.05 |
| NIN ⁴⁴ | - | 8.81 | 35.68 |
| Single-Objective Approaches | | | |
| Genetic CNN ⁹¹ | - | 7.10 | 29.05 |
| Block-QNN ⁹⁷ | 39.8 | 3.50 | - |
| Block-QNN-s ⁹⁷ | 6.1 | 4.38 | 20.65 |
| LaNet-S ⁹⁰ | 3.2 | 1.63 | - |
| LaNet-L ⁹⁰ | 44.1 | 0.99 | - |
| oneshot-LaNet-S ⁹⁰ | 3.6 | 1.68 | - |
| oneshot-LaNet-L ⁹⁰ | 45.3 | 1.20 | - |
| Large-scale Evolution ⁶³ | 5.4 | 5.40 | - |
| | 40.4 | - | 23.00 |
| MetaQNN ⁹ | - | 6.92 | 27.14 |
| AE-CNN ⁸⁰ | 2.0 | 4.30 | - |
| | 5.4 | - | 20.85 |
| Multi-Objective Approaches | | | |
| NSGA-Net ⁵⁰ | 0.2 | 4.67 | - |
| | 4.0 | 2.02 | - |
| | 0.2 | - | 25.17 |
| | 4.1 | - | 14.38 |
| MOGIG-Net | 0.9 | 4.67 | - |
| | 3.0 | 3.13 | - |
| | 3.7 | 2.01 | - |
| | 0.7 | - | 24.71 |
| | 3.2 | - | 18.23 |
| | 3.7 | - | 14.38 |

708 Since numerical results indicate that the proposed MOGIG-Net is able to design excellent CNNs, a future direction of our research will include the extension of the encoding strategy to other ingenious neural systems recently proposed in the literature, such as Enhanced Probabilistic Neural Network⁵, Neural Dynamic Classification Algorithm⁶¹, Dynamic Ensemble Learning Algorithm⁶, and Finite Element Machine for Fast Learning⁶⁰

718 5. Conclusion

719 This paper proposes a NAS method to design CNNs with high performance in terms of accuracy and a limited impact on the computational resources.

720 The proposed algorithm indicated with MOGIG-Net makes use of a novel block logic based on adjacency list to compose the network structure. The encoding mechanism proposed in this paper can naturally represent the structure of any graph. Moreover, MOGIG-Net employs ad-hoc crossover and mutation operators which are designed to explore the search space and identify potential candidate structures. At last, the proposed network encoding enables that the parent structures can be effectively and naturally transferred to the offspring during the crossover process. The proposed approach overcomes the limitation of classical NAS approaches based on Evolutionary Algorithms which require a search in a large space and an overhead due to multiple re-training sessions. Numerical results on two popular datasets Cifar-10 and Cifar-100 show that MOGIG-Net can exceed most existing network structures.

741 This paper confirms that multi-objective optimization modelling is a promising direction of research in the field of NAS. Future research will consider further objectives and strategies to reduce the computational cost of the training by e.g. limiting the number of skip connections in the first generation.

748 Acknowledgment

749 This work was partially supported by the National Natural Science Foundation of China (61876089, 61876185, 61902281), the opening Project of Jiangsu Key Laboratory of Data Science and Smart Software (No.2019DS301), the Natural Science Foundation of

Jiangsu Province (BK20141005), the Natural Science Foundation of the Jiangsu Higher Education Institutions of China (14KJB520025).

References

1. H. A. Abbass, Pareto neuro-evolution: Constructing ensemble of neural networks using multi-objective optimization, *IEEE Congress on Evolutionary Computation*, 3 2003, pp. 2074–2080.
2. U. R. Acharya, S. L. Oh, Y. Hagiwara, J. H. Tan and H. Adeli, Deep convolutional neural network for the automated detection and diagnosis of seizure using eeg signals, *Computers in biology and medicine* **100** (2018) 270–278.
3. U. R. Acharya, S. L. Oh, Y. Hagiwara, J. H. Tan, H. Adeli and D. P. Subha, Automated eeg-based screening of depression using deep convolutional neural network, *Computer methods and programs in biomedicine* **161** (2018) 103–113.
4. A. Agogino, K. Stanley and R. Miikkulainen, Online interactive neuro-evolution, *Neural Processing Letters* **11**(1) (2000) 29–38.
5. M. Ahmadlou and H. Adeli, Enhanced probabilistic neural network with local decision circles: A robust classifier, *Integrated Computer-Aided Engineering* **17**(3) (2010) 197–210.
6. K. M. R. Alam, N. Siddique and H. Adeli, A dynamic ensemble learning algorithm for neural networks, *Neural Computing and Applications* **32**(12) (2020) 8675–8690.
7. A. H. Ansari, P. J. Cherian, A. Caicedo, G. Naulaers, M. De Vos and S. Van Huffel, Neonatal seizure detection using deep convolutional neural networks, *International journal of neural systems* **29**(04) (2019) p. 1850011.
8. A. Asseman, N. Antoine and A. S. Ozcan, Accelerating deep neuroevolution on distributed fpgas for reinforcement learning problems, *ACM Journal on Emerging Technologies in Computing Systems (JETC)* **17**(2) (2021) 1–17.
9. B. Baker, O. Gupta, N. Naik and R. Raskar, Designing neural network architectures using reinforcement learning, *International Conference on Learning Representations*, 2017.
10. B. Baker, O. Gupta, R. Raskar and N. Naik, Accelerating neural architecture search using performance prediction, *International Conference on Learning Representations*, 2018.
11. G. Bender, P.-J. Kindermans, B. Zoph, V. Vasudevan and Q. Le, Understanding and simplifying one-shot architecture search, *International Conference on Machine Learning*, 2018, pp. 550–559.
12. S. Bhat, U. R. Acharya, Y. Hagiwara, N. Dadmehr and H. Adeli, Parkinson’s disease: Cause factors, measurable indicators, and early diagnosis, *Computers in biology and medicine* **102** (2018) 234–241.
13. C. Blum, R. Chiong, M. Clerc, K. De Jong, Z. Michalewicz, F. Neri and T. Weise, Evolutionary optimization, *Variants of evolutionary algorithms for real-world applications*, (Springer, 2012), pp. 1–29.
14. H. Cai, J. Yang, W. Zhang, S. Han and Y. Yu, Path-level network transformation for efficient architecture search, *PMLR International Conference on Machine Learning*, 2018, pp. 678–687.
15. H. Cai, L. Zhu and S. Han, Proxylessnas: Direct neural architecture search on target task and hardware, *International Conference on Learning Representations*, 2018.
16. X. Cao, J. Yao, Z. Xu and D. Meng, Hyperspectral image classification with convolutional neural network and active learning, *IEEE Transactions on Geoscience and Remote Sensing* **58**(7) (2020) 4604–4616.
17. F. Charte, A. J. Rivera, F. Martínez and M. J. del Jesus, Evoaaa: An evolutionary methodology for automated neural autoencoder architecture search, *Integrated Computer-Aided Engineering* (Preprint) (2020) 1–21.
18. L.-C. Chen, M. Collins, Y. Zhu, G. Papandreou, B. Zoph, F. Schroff, H. Adam and J. Shlens, Searching for efficient multi-scale architectures for dense image prediction, *Advances in neural information processing systems*, 2018, pp. 8699–8710.
19. F. Chollet, Xception: Deep learning with depthwise separable convolutions, *Proceedings of the IEEE conference on computer vision and pattern recognition*, 2017, pp. 1251–1258.
20. X. Dai, P. Zhang, B. Wu, H. Yin, F. Sun, Y. Wang, M. Dukhan, Y. Hu, Y. Wu, Y. Jia *et al.*, Chamnet: Towards efficient network design through platform-aware model adaptation, *Proceedings of the IEEE Conference on computer vision and pattern recognition*, 2019, pp. 11398–11407.
21. A. Diba, A. Pazandeh and L. Van Gool, Efficient two-stream motion and appearance 3d cnns for video classification, *Proceedings*, 2016, pp. 1–4.
22. X. Dong and Y. Yang, One-shot neural architecture search via self-evaluated template network, *Proceedings of the IEEE/CVF International Conference on Computer Vision*, 2019, pp. 3681–3690.
23. T. Elsken, J. H. Metzen and F. Hutter, Efficient multi-objective neural architecture search via lamarckian evolution, *International Conference on Learning Representations*, 2018.
24. T. Elsken, J.-H. Metzen and F. Hutter, Simple and efficient architecture search for convolutional neural networks, *International Conference on Learning Representations*, 2018.
25. J. Fang, Y. Sun, Q. Zhang, Y. Li, W. Liu and X. Wang, Densely connected search space for more flexible neural architecture search, *Proceedings of the IEEE/CVF Conference on Computer Vision and Pattern Recognition*, 2020, pp. 10628–10637.
26. F. Gomez, J. Schmidhuber and R. Miikkulainen, Efficient non-linear control through neuroevolution, *European Conference on Machine Learning*, (Springer,

- 2006), pp. 654–662.
- 869 27. F. J. Gomez and R. Miikkulainen, Solving non-
870 markovian control tasks with neuroevolution, *IJCAI*,
871 **99** 1999, pp. 1356–1361.
- 872 28. X. Gong, S. Chang, Y. Jiang and Z. Wang, Autogan:
873 Neural architecture search for generative adversarial
874 networks, *Proceedings of the IEEE International Confer-
875 ence on Computer Vision*, 2019, pp. 3224–3234.
- 876 29. Z. Guo, X. Zhang, H. Mu, W. Heng, Z. Liu, Y. Wei and
877 J. Sun, Single path one-shot neural architecture search
878 with uniform sampling, *European Conference on Com-
879 puter Vision*, (Springer, 2020), pp. 544–560.
- 880 30. M. Hausknecht, J. Lehman, R. Miikkulainen and
881 P. Stone, A neuroevolution approach to general atari
882 game playing, *IEEE Transactions on Computational In-
883 telligence and AI in Games* **6**(4) (2014) 355–366.
- 884 31. K. He, X. Zhang, S. Ren and J. Sun, Deep residual
885 learning for image recognition, *Proceedings of the IEEE
886 conference on computer vision and pattern recognition*,
887 2016, pp. 770–778.
- 888 32. O. M. Hooman, M. M. Al-Rifaie and M. A. Nicolaou,
889 Deep neuroevolution: Training deep neural networks
890 for false alarm detection in intensive care units, *2018
891 26th IEEE European Signal Processing Conference (EU-
892 SIPCO)*, 2018, pp. 1157–1161.
- 893 33. G. Huang, Z. Liu, L. Van Der Maaten and K. Q. Wein-
894 berger, Densely connected convolutional networks,
895 *Proceedings of the IEEE conference on computer vision
896 and pattern recognition*, 2017, pp. 4700–4708.
- 897 34. H. Jiang, F. Gao, X. Xu, F. Huang and S. Zhu, Atten-
898 tive and ensemble 3d dual path networks for pul-
899 monary nodules classification, *Neurocomputing* **398**
900 (2020) 422–430.
- 901 35. N. Karthikeyan and R. Sukanesh, Cloud based emer-
902 gency health care information service in india, *Journal
903 of medical systems* **36**(6) (2012) 4031–4036.
- 904 36. A. Krizhevsky, One weird trick for parallelizing con-
905 volutional neural networks, tech. report (2014).
- 906 37. A. Krizhevsky, G. Hinton and others, Learning mul-
907 tiple layers of features from tiny images, tech. report,
908 University of Toronto (2009).
- 909 38. H. Kwasnicka and M. Paradowski, Efficiency aspects
910 of neural network architecture evolution using direct
911 and indirect encoding, *Adaptive and Natural Comput-
912 ing Algorithms*, (Springer, 2005), pp. 405–408.
- 913 39. S. Li, X. Zhao and G. Zhou, Automatic pixel-level
914 multiple damage detection of concrete structure us-
915 ing fully convolutional network, *Computer-Aided Civil
916 and Infrastructure Engineering* **34**(7) (2019) 616–634.
- 917 40. X. Li, Y. Jiang, M. Li and S. Yin, Lightweight attention
918 convolutional neural network for retinal vessel im-
919 age segmentation, *IEEE Transactions on Industrial In-
920 formatics* **17**(3) (2020) 1958–1967.
- 921 41. X. Li, C. Lin, C. Li, M. Sun, W. Wu, J. Yan and
922 W. Ouyang, Improving one-shot nas by suppress-
923 ing the posterior fading, *Proceedings of the IEEE/CVF
924 Conference on Computer Vision and Pattern Recognition*,
925 2020, pp. 13836–13845.
- 926 42. Y. Li, Z. Yu, Y. Chen, C. Yang, Y. Li, X. Allen Li and
927 B. Li, Automatic seizure detection using fully convo-
928 lutional nested lstm, *International journal of neural sys-
929 tems* **30**(04) (2020) p. 2050019.
- 930 43. L.-C. Lin, C.-S. Ouyang, R.-C. Wu, R.-C. Yang and
931 C.-T. Chiang, Alternative diagnosis of epilepsy in
932 children without epileptiform discharges using deep
933 convolutional neural networks, *International journal of
934 neural systems* **30**(05) (2020) p. 1850060.
- 935 44. M. Lin, Q. Chen and S. Yan, Network in network,
936 *International Conference on Learning Representations*,
937 2014.
- 938 45. C. Liu, B. Zoph, M. Neumann, J. Shlens, W. Hua, L.-J.
939 Li, L. Fei-Fei, A. Yuille, J. Huang and K. Murphy, Pro-
940 gressive neural architecture search, *Proceedings of the
941 European Conference on Computer Vision (ECCV)*, 2018,
942 pp. 19–34.
- 943 46. G. Liu, W. Zhou and M. Geng, Automatic seizure de-
944 tection based on s-transform and deep convolutional
945 neural network, *International journal of neural systems*
946 **30**(04) (2020) p. 1950024.
- 947 47. H. Liu, K. Simonyan and Y. Yang, Darts: Differen-
948 tiable architecture search, *International Conference on
949 Learning Representations*, 2018.
- 950 48. Z. Liu, Z. Wu, T. Li, J. Li and C. Shen, Gmm and cnn
951 hybrid method for short utterance speaker recogni-
952 tion, *IEEE Transactions on Industrial informatics* **14**(7)
953 (2018) 3244–3252.
- 954 49. Z. Lu, K. Deb and V. N. Boddeti, MUXConv: Infor-
955 mation Multiplexing in Convolutional Neural Net-
956 works, *Proceedings of the IEEE/CVF Conference on Com-
957 puter Vision and Pattern Recognition*, 2020, pp. 12044–
958 12053.
- 959 50. Z. Lu, I. Whalen, V. Boddeti, Y. Dhebar, K. Deb,
960 E. Goodman and W. Banzhaf, Nsga-net: neural ar-
961 chitecture search using multi-objective genetic algo-
962 rithm, *Proceedings of the Genetic and Evolutionary Com-
963 putation Conference*, 2019, pp. 419–427.
- 964 51. N. Ma, X. Zhang, H.-T. Zheng and J. Sun, Shufflenet
965 v2: Practical guidelines for efficient cnn architecture
966 design, *Proceedings of the European conference on com-
967 puter vision (ECCV)*, 2018, pp. 116–131.
- 968 52. Z. Ma, Reachability analysis of neural masses and
969 seizure control based on combination convolutional
970 neural network, *International journal of neural systems*
971 **30**(01) (2020) p. 1950023.
- 972 53. K. Maeda, S. Takahashi, T. Ogawa and M. Haseyama,
973 Convolutional sparse coding-based deep random
974 vector functional link network for distress classifica-
975 tion of road structures, *Computer-Aided Civil and In-
976 frastructure Engineering* **34**(8) (2019) 654–676.
- 977 54. O. M. Manzanera, S. K. Meles, K. L. Leenders, R. J.
978 Renken, M. Pagani, D. Arnaldi, F. Nobili, J. Obeso,
979 M. R. Oroz, S. Morbelli and N. M. Mauritis, Scaled
980 subprofile modeling and convolutional neural net-
981 works for the identification of parkinson’s disease in
982 3d nuclear imaging data, *International journal of neural
983 systems* **29**(09) (2019) p. 1950010.

55. H. Mo, L. L. Custode and G. Iacca, Evolutionary neural architecture search for remaining useful life prediction, *Applied Soft Computing* **108** (2021) p. 107474. 984
56. H. Mo, F. Lucca, J. Malacarne and G. Iacca, Multi-head cnn-lstm with prediction error analysis for remaining useful life prediction, *2020 27th Conference of Open Innovations Association (FRUCT)*, (IEEE, 2020), pp. 164–171. 985
57. R. Negrinho, M. Gormley, G. J. Gordon, D. Patil, N. Le and D. Ferreira, Towards modular and programmable architecture search, *Advances in Neural Information Processing Systems*, 2019, pp. 13715–13725. 986
58. F. Neri, *Linear Algebra for Computational Sciences and Engineering*, second edn. (Springer, 2019). 987
59. B. K. Oh, B. Glisic, Y. Kim and H. S. Park, Convolutional neural network-based wind-induced response estimation model for tall buildings, *Computer-Aided Civil and Infrastructure Engineering* **34**(10) (2019) 843–858. 988
60. D. R. Pereira, M. A. Piteri, A. N. Souza, J. P. Papa and H. Adeli, Fema: a finite element machine for fast learning, *Neural Computing and Applications* **32**(10) (2020) 6393–6404. 989
61. M. H. Rafiei and H. Adeli, A new neural dynamic classification algorithm, *IEEE transactions on neural networks and learning systems* **28**(12) (2017) 3074–3083. 990
62. E. Real, A. Aggarwal, Y. Huang and Q. V. Le, Regularized evolution for image classifier architecture search, *Proceedings of the aaai conference on artificial intelligence*, **33**(01) 2019, pp. 4780–4789. 991
63. E. Real, S. Moore, A. Selle, S. Saxena, Y. L. Suematsu, J. Tan, Q. V. Le and A. Kurakin, Large-scale evolution of image classifiers, *International Conference on Machine Learning*, 2017, pp. 2902–2911. 992
64. S. Risi and K. O. Stanley, Deep neuroevolution of recurrent and discrete world models, *Proceedings of the Genetic and Evolutionary Computation Conference*, 2019, pp. 456–462. 993
65. S. Rostami, F. Neri and M. Epitropakis, Progressive preference articulation for decision making in multi-objective optimisation problems, *Integrated Computer-Aided Engineering* **24**(4) (2017) 315–335. 994
66. S. Rostami, F. Neri and K. Gyaurski, On algorithmic descriptions and software implementations for multi-objective optimisation: A comparative study, *SN Computer Science* **1**(5) (2020) 1–23. 995
67. C. Saltori, S. Roy, N. Sebe and G. Iacca, Regularized evolutionary algorithm for dynamic neural topology search, *International Conference on Image Analysis and Processing*, (Springer, 2019), pp. 219–230. 996
68. M. Sandler, A. Howard, M. Zhu, A. Zhmoginov and L.-C. Chen, Mobilenetv2: Inverted residuals and linear bottlenecks, *Proceedings of the IEEE conference on computer vision and pattern recognition*, 2018, pp. 4510–4520. 997
69. K. C. Sarma and H. Adeli, Fuzzy discrete multicriteria cost optimization of steel structures, *Journal of structural engineering* **126**(11) (2000) 1339–1347. 998
70. K. C. Sarma and H. Adeli, Bilevel parallel genetic algorithms for optimization of large steel structures, *Computer-Aided Civil and Infrastructure Engineering* **16**(5) (2001) 295–304. 999
71. W. W. Seeley, J. M. Allman, D. A. Carlin, R. K. Crawford, M. N. Macedo, M. D. Greicius, S. J. Dearmond and B. L. Miller, Divergent social functioning in behavioral variant frontotemporal dementia and alzheimer disease: reciprocal networks and neuronal evolution, *Alzheimer Disease & Associated Disorders* **21**(4) (2007) S50–S57. 1000
72. J. Shen, X. Xiong, Z. Xue and Y. Bian, A convolutional neural-network-based pedestrian counting model for various crowded scenes, *Computer-Aided Civil and Infrastructure Engineering* **34**(10) (2019) 897–914. 1001
73. W. Shin, S.-J. Bu and S.-B. Cho, 3d-convolutional neural network with generative adversarial network and autoencoder for robust anomaly detection in video surveillance, *International Journal of Neural Systems* **30**(06) (2020) p. 2050034. 1002
74. K. Simonyan and A. Zisserman, Very deep convolutional networks for large-scale image recognition, *International Conference on Learning Representations*, 2015. 1003
75. M. G. Soto and H. Adeli, Many-objective control optimization of high-rise building structures using replicator dynamics and neural dynamics model, *Structural and Multidisciplinary Optimization* **56**(6) (2017) 1521–1537. 1004
76. K. O. Stanley, J. Clune, J. Lehman and R. Miikkulainen, Designing neural networks through neuroevolution, *Nature Machine Intelligence* **1**(1) (2019) 24–35. 1005
77. F. P. Such, V. Madhavan, E. Conti, J. Lehman, K. O. Stanley and J. Clune, Deep neuroevolution: Genetic algorithms are a competitive alternative for training deep neural networks for reinforcement learning, *International Conference on Learning Representations*, 2019. 1006
78. Y. Sun, H. Wang, B. Xue, Y. Jin, G. G. Yen and M. Zhang, Surrogate-assisted evolutionary deep learning using an end-to-end random forest-based performance predictor, *IEEE Transactions on Evolutionary Computation* **24**(2) (2019) 350–364. 1007
79. Y. Sun, B. Xue, M. Zhang and G. G. Yen, A particle swarm optimization-based flexible convolutional autoencoder for image classification, *IEEE transactions on neural networks and learning systems* **30**(8) (2018) 2295–2309. 1008
80. Y. Sun, B. Xue, M. Zhang and G. G. Yen, Completely automated CNN architecture design based on blocks, *IEEE transactions on neural networks and learning systems* **31**(4) (2019) 1242–1254, Publisher: IEEE. 1009
81. Y. Sun, B. Xue, M. Zhang and G. G. Yen, Evolving deep convolutional neural networks for image classification, *IEEE Transactions on Evolutionary Computation* **24**(2) (2019) 394–407, Publisher: IEEE. 1010
82. Y. Sun, B. Xue, M. Zhang, G. G. Yen and J. Lv, Au- 1011

- 1100 automatically designing cnn architectures using the ge- 1138
 1101 netic algorithm for image classification, *IEEE Transac-* 1139
 1102 *tions on Cybernetics* (2020). 1140
 1103 83. C. Szegedy, S. Ioffe, V. Vanhoucke and A. A. Alemi, 1141
 1104 Inception-v4, inception-resnet and the impact of 1142
 1105 residual connections on learning, *Proceedings of the* 1143
 1106 *Thirty-First AAAI Conference on Artificial Intelligence,* 1144
 1107 2017, pp. 4278–4284. 1145
 1108 84. C. Szegedy, W. Liu, Y. Jia, P. Sermanet, S. Reed, 1146
 1109 D. Anguelov, D. Erhan, V. Vanhoucke and A. Rabi- 1147
 1110 novich, Going deeper with convolutions, *Proceedings* 1148
 1111 *of the IEEE conference on computer vision and pattern* 1149
 1112 *recognition*, 2015, pp. 1–9. 1150
 1113 85. M. Tan, B. Chen, R. Pang, V. Vasudevan, M. Sandler, 1151
 1114 A. Howard and Q. V. Le, Mnasnet: Platform-aware 1152
 1115 neural architecture search for mobile, *Proceedings of* 1153
 1116 *the IEEE Conference on Computer Vision and Pattern* 1154
 1117 *Recognition*, 2019, pp. 2820–2828. 1155
 1118 86. M. Tan and Q. Le, Efficientnet: Rethinking model 1156
 1119 scaling for convolutional neural networks, *Interna-* 1157
 1120 *tional Conference on Machine Learning*, 2019, pp. 6105– 1158
 1121 6114. 1159
 1122 87. M. Tan and Q. V. Le, Mixconv: Mixed depthwise con- 1160
 1123 volutional kernels, *30th British Machine Vision Con-* 1161
 1124 *ference 2019, BMVC 2019, Cardiff, UK, September 9-12,* 1162
 1125 *2019*, (BMVA Press, 2019), p. 74. 1163
 1126 88. K. Thurnhofer-Hemsi, E. López-Rubio, N. Roe-Vellve 1164
 1127 and M. A. Molina-Cabello, Multiobjective optimiza- 1165
 1128 tion of deep neural networks with combinations 1166
 1129 of lp-norm cost functions for 3d medical image 1167
 1130 super-resolution, *Integrated Computer-Aided Engineer-* 1168
 1131 *ing* (Preprint) (2020) 1–19. 1169
 1132 89. B. Wang, Y. Sun, B. Xue and M. Zhang, Evolving deep 1170
 1133 neural networks by multi-objective particle swarm 1171
 1134 optimization for image classification, *Proceedings of* 1172
 1135 *the Genetic and Evolutionary Computation Conference,* 1173
 1136 2019, pp. 490–498. 1174
 1137 90. L. Wang, S. Xie, T. Li, R. Fonseca and Y. Tian, Sample-
 efficient neural architecture search by learning ac-
 tions for monte carlo tree search, *IEEE Transactions on*
Pattern Analysis and Machine Intelligence (2021) 1–1, to
 appear.
 91. L. Xie and A. Yuille, Genetic cnn, *Proceedings of the*
IEEE international conference on computer vision, 2017,
 pp. 1379–1388.
 92. S. Xie, H. Zheng, C. Liu and L. Lin, Snas: stochastic
 neural architecture search, *International Conference on*
Learning Representations, 2018.
 93. Y. Xue, Y. Tang, X. Xu, J. Liang and F. Neri, Multi-
 objective feature selection with missing data in classi-
 fication, *IEEE Transactions on Emerging Topics in Com-*
putational Intelligence (2021).
 94. X. Yao and M. M. Islam, Evolving artificial neural net-
 work ensembles, *IEEE Computational Intelligence Mag-*
azine 3(1) (2008) 31–42.
 95. Y. Zhang,
 Y. Miyamori, S. Mikami and T. Saito, Vibration-based
 structural state identification by a 1-dimensional con-
 volutional neural network, *Computer-Aided Civil and*
Infrastructure Engineering 34(9) (2019) 822–839.
 96. D. Zhipeng, W. Jingcheng, X. Yumin, M. Qingmin
 and W. Xiaoming, Voiceprint recognition based on bp
 neural network and cnn, *Journal of Physics: Conference*
Series, 1237(3) 2019, p. 032032.
 97. Z. Zhong, J. Yan and C.-L. Liu, Practical net-
 work blocks design with q-learning, *arXiv preprint*
arXiv:1708.05552 1(2) (2017) p. 5.
 98. B. Zoph and Q. V. Le, Neural architecture search
 with reinforcement learning, *International Conference*
on Learning Representations, 2017.
 99. B. Zoph, V. Vasudevan, J. Shlens and Q. V. Le,
 Learning transferable architectures for scalable im-
 age recognition, *Proceedings of the IEEE conference on*
computer vision and pattern recognition, 2018, pp. 8697–
 8710.